Tuning Optoelectronic Properties of Ambipolar Organic Light-Emitting Transistors Using a Bulk-Heterojunction Approach

Loi, Maria Antonietta; Rost-Bietsch, Constance; Murgia, Mauro; Karg, Siegfried; Riess, Walter; Muccini, Michele

Published in:
Advanced Functional Materials

DOI:
10.1002/adfm.200500424

DOI: 10.1002/adfm.200500424

Tuning Optoelectronic Properties of Ambipolar Organic Light-Emitting Transistors Using a Bulk-Heterojunction Approach**

By *Maria Antonietta Loi*,* *Constance Rost-Bietsch*, *Mauro Murgia*, *Siegfried Karg*, *Walter Riess*, and *Michele Muccini*

Bulk-heterojunction engineering is demonstrated as an approach to producing ambipolar organic light-emitting field-effect transistors with tunable electrical and optoelectronic characteristics. The electron and hole mobilities, as well as the electroluminescence intensity, can be tuned over a large range by changing the composition of a bimolecular mixture consisting of α-quinquethiophene and *N,N′*-ditridecylperylene-3,4,9,10-tetracarboxylic-diimide. Time-resolved photoluminescence spectroscopy reveals that the phase segregation of the two molecules in the bulk heterojunction and their electronic interaction determine the optoelectronic properties of the devices. The results presented show that the bulk-heterojunction approach, which is widely used in organic photovoltaic cells, can be successfully employed to select and tailor the functionality of field-effect devices, including ambipolar charge transport and light emission.

1. Introduction

In the past decades, the development of organic-material-based devices, such as light-emitting diodes (LEDs),[1,2] solar cells,[3,4] electrochemical cells,[5] organic memories,[6,7] and field-effect transistors (FETs)[8–11] was driven by the great advancements made in organic materials science. The performance of organic LEDs has been advanced to such an extent that they can be driven by amorphous-silicon thin-film-transistor backplanes in active-matrix displays.[12] The mobility of organic FETs is now comparable to that of amorphous-silicon FETs (about 1 $cm^2 V^{-1} s^{-1}$). Consequently, organic FETs can now be developed as switching devices for active-matrix LED displays,[13] low-cost, large-area flexible microelectronics,[14–16] and hybrid electronics.[12] The combination in a single device of two functionalities, such as electrical switching and light emission, increases the number of applications of organic semiconductors and is a step towards realizing the idea of completely integrated organic optoelectronics.[11]

Recently, the production of light-emitting FETs (LETs) with unipolar electrical characteristics (p-type transport) based on molecular semiconductors[17,18] and polymers[19,20] was reported. Ambipolar charge transport is a desirable property for organic semiconductors as it enables the fabrication of complementary logic circuits such as CMOS (CMOS: complementary metal oxide semiconductor) transistors with a single active layer.[21,22] Moreover, ambipolar conduction is crucial in LETs for maximizing exciton recombination through electron–hole balancing, as well as for adjusting the position of the recombination region in the channel by tuning the gate voltage.[23]

From a theoretical viewpoint, pure organic semiconductors should support both electron and hole conduction equally.[24] In practice, organic semiconductors favor unipolar charge transport, and the majority of them are p-type.[25] Only few ambipolar organic materials are known, and their mobilities do not exceed 10^{-4} to 10^{-5} $cm^2 V^{-1} s^{-1}$.[22,26] Their limited number and moderate mobility stimulated the search for alternative approaches to achieving ambipolar transport in FETs.[27–29] As an approach of general importance for organic semiconductors, the formation of bulk heterojunctions was demonstrated to be a viable way to fabricate LEDs[30,31] and solar cells.[3,32] Bulk heterojunctions of solution-processed blends of a hole-transporting polymer and electron-transporting molecules, such as fullerene and perylene, were reported to yield ambipolar conduction in FET configuration.[22,29,33] Field-effect mobility values of up to 10^{-3} $cm^2 V^{-1} s^{-1}$ have been obtained, but light emission from such FETs was not observed prior to our report of the first ambipolar organic LET.[34] In that work, the active layer consisted of a vacuum-sublimed bulk heterojunction composed of *N,N′*-ditridecylperylene-3,4,9,10-tetracarboxylic diimide (P13) for electron conduction and α-quinquethiophene (T5) for hole conduction. T5 is known as a good hole-trans-

[*] Dr. M. A. Loi, Dr. M. Murgia, Dr. M. Muccini
Istituto per lo Studio dei Materiali Nanostrutturati (ISMN)
Consiglio Nazionale delle Ricerche (CNR)
via P. Gobetti 101, I-40129 Bologna (Italy)
E-mail: MA.Loi@bo.ismn.cnr.it
Dr. C. Rost-Bietsch, Dr. S. Karg, Dr. W. Riess
IBM Research GmbH
Säumerstrasse 4, CH-8803 Rüschlikon (Switzerland)

[**] The authors thank M. Melucci and G. Barbarella (CNR-ISOF Bologna) for providing T5. Fruitful discussions with V. A. L. Roy, E. Da Como and R. Zamboni (CNR-ISMN Bologna) are also acknowledged. Research supported by the EU-IST-FET program under project IST-33057 (ILO) and the Italian Ministry MIUR under Project FIRB-RBNE033KMA.

porting material,[35] and P13 belongs to a class of perylene derivatives, which are well-studied electron-transporting materials.[36] The molecular structures of T5 and P13 and a schematic of the device architecture are shown in Figure 1. For reference, pure devices of T5 and P13 were fabricated, and hole and electron mobilities of 2.5×10^{-2} and 1×10^{-2} $cm^2 V^{-1} s^{-1}$, respectively, were extracted.

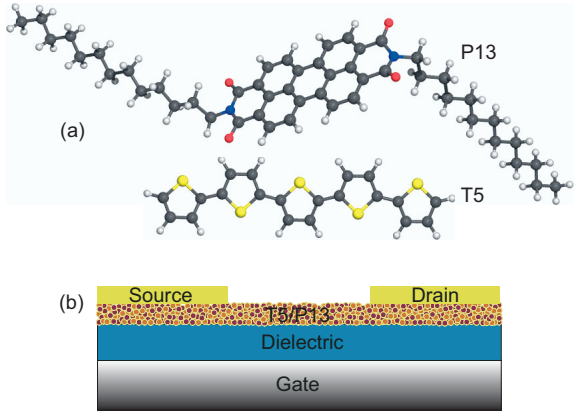

Figure 1. a) Molecular structure of P13 and T5, and b) schematic cross-section of the FET device based on the co-evaporated thin film of P13 and T5.

The two materials were chosen because the relative positions of their highest occupied and the lowest unoccupied molecular orbitals (HOMO and LUMO, respectively) allow exciton formation and recombination in the material with the smaller energy gap.[34] The HOMO level of T5 lies at about –5.3 eV[37] and the LUMO level at about –2.8 eV.[37] The HOMO and the LUMO levels of P13 are estimated to be ~–5.4 and ~–3.4 eV,[38] respectively.

Here we demonstrate that the approach of bulk-heterojunction engineering permits fine tuning of both the electron and hole mobility, as well as of the electroluminescence (EL) intensity in field-effect devices. By controlled co-evaporation of T5 and P13, we are able to adjust both the electron and the hole field-effect mobility over two orders of magnitude (10^{-4}–10^{-2} $cm^2 V^{-1} s^{-1}$). The EL intensity is also determined by the relative concentration of materials and by the structural features of the bulk heterojunction.

In particular, we are able to identify three different working regimes of the ambipolar light-emitting field-effect devices by varying the volume ratio of the constituents of the bulk heterojunction. The first regime is obtained for bulk heterojunctions composed of an excess of T5 and is characterized by ambipolar electrical conduction and absence of light emission. In the second working regime, the active layer has a balanced material composition and exhibits ambipolar electrical properties accompanied by light emission. For bulk heterojunctions composed of an excess of P13, the third regime is obtained. It is characterized by unipolar electron transport and light emission.

The electronic transport and EL properties of the bulk-heterojunction LETs are discussed by investigating the film morphology and recombination processes of the excited states by means of confocal laser scanning microscopy (CLSM) and time-resolved photoluminescence (PL) spectroscopy.

2. Results and Discussion

Figure 2 shows the output (Fig. 2a) and transfer (Fig. 2b) characteristics, with their corresponding EL intensities, for a bulk-heterojunction LET composed of T5 and P13 in a 1:1 vol-

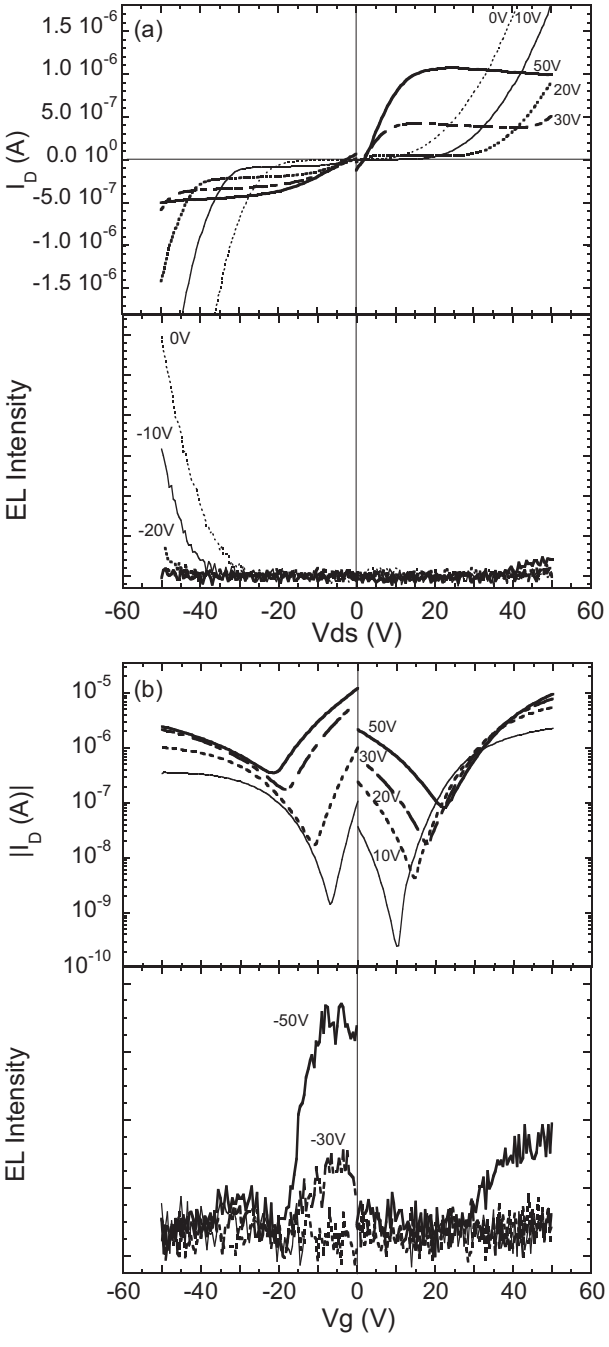

Figure 2. a) Output and b) transfer characteristics, showing drain current (I_D) and corresponding EL intensity, of a transistor with a T5/P13 ratio of 1:1. Adapted from [34].

ume ratio. The transistor exhibits a pronounced ambipolar behavior in the output and transfer characteristics, as discussed in detail in a previous publication[34]. From the transfer curves, a hole mobility of 5×10^{-4} cm^2 V^{-1} s^{-1} and an electron mobility of 1×10^{-3} cm^2 V^{-1} s^{-1} are extracted. In the output characteristics for negative source–drain voltage, V_{DS}, and gate voltage, V_G, the light output is apparently correlated with the non-saturating drain current. The highest brightness is achieved for $V_G = 0$ V and $V_{DS} = -50$ V, and the intensity decreases with increasing $|V_G|$. The onset and magnitude correlate well with the drain current, whereas for positive bias voltages only weak emission is observed and no obvious correlation with the drain current seems to exist.

In the transfer characteristics, the EL shows a maximum for intermediate V_G. The position of the maximum shifts with increasing $|V_{DS}|$ to larger values of $|V_G|$, and the intensity increases with increasing $|V_{DS}|$. One would expect that the maximum occurs at $V_G = 0.5\, V_{DS}$ as there is an equal potential drop for electron and hole injection, leading to a maximum in the *np* product (*n*: electron density; *p*: hole density) of injected charge-carrier densities. According to Langevin recombination[39] the EL intensity, *I*, scales as $I \propto np(\mu_n + \mu_p)$. The actual position of the EL maximum is shifted by the threshold voltages of the n- and p-channel transistor operation.

To investigate the influence of the composition of the bulk heterojunction on the mobility and EL intensity, transistors with a systematic variation in the T5/P13 volume ratio have been investigated. The devices with an excess of P13, e.g., those with T5/P13 ratios of 1:3 and 1:9, exhibit both light emission and unipolar electron current. Output and transfer characteristics of the transistor with a T5/P13 ratio of 1:3 are shown in Figure 3, together with its corresponding EL intensity. Although the output characteristics show no indication of ambipolar transport, EL occurs for both polarities of V_{DS}. The EL onset $|V_{DS}|$ increases with increasing $|V_G|$, as does the slope, resulting in a crossing of EL curves corresponding to different values of V_G. In the transfer characteristics, the EL maximum still occurs at about $V_G = 0.5\, V_{DS}$. At first glance, the observation of EL in a unipolar device seems to be counterintuitive. However, holes are still injected even though their mobility is low and their contribution to the overall current is negligible. According to the Langevin relation, EL occurs if both types of carriers are injected and at least one of them exhibits a non-zero mobility.

The devices with an excess of T5, e.g., those with T5/P13 ratios of 3:1 and 9:1, show ambipolar charge-carrier transport, but no light emission. From the sample with a ratio of 3:1, an electron field-effect mobility of 9×10^{-4} cm^2 V^{-1} s^{-1} and a hole field-effect mobility of 3×10^{-3} cm^2 V^{-1} s^{-1} were obtained.

In Figure 4 the extracted mobilities of the different compositions of the T5/P13 bulk heterojunction are depicted. In addition, the mobilities of pure reference devices has been included. Both the electron and the hole mobility decrease exponentially when the relative concentrations of the electron- and the hole-transporting material are decreased from 100 to 50 %. The electron mobility decreases in this range by one order of magnitude, whereas the hole mobility decreases by

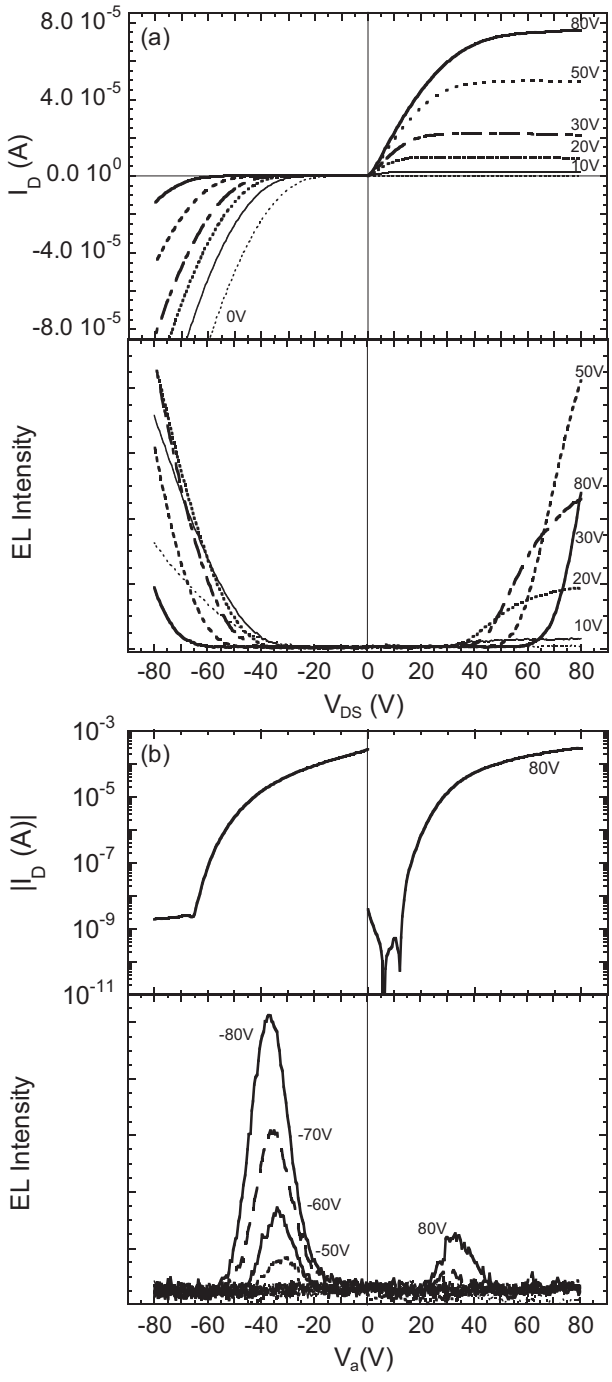

Figure 3. a) Output and b) transfer characteristics, showing I_D and corresponding EL intensity, of a transistor with a T5/P13 ratio of 1:3.

1.5 orders of magnitude. At lower concentrations, the electron mobility seems to level off, whereas the hole mobility is below the detection limit. Electron as well as hole mobility, i.e., ambipolar transport, on the same sample could only be measured for devices that had T5/P13 ratios of 1:1 and 3:1. A perfect balance of the electron and the hole mobility is extrapolated for a bulk heterojunction with a T5/P13 ratio of roughly 3:2.

Figure 5 compares the EL intensity as a function of the drain current for devices with different volume ratios at $V_{DS} = 0$ and

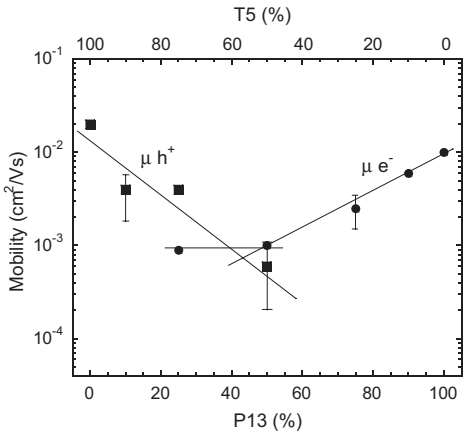

Figure 4. Electron (filled circles) and hole (filled squares) field-effect mobilities for different bulk-heterojunction compositions. The lines are guides to the eye.

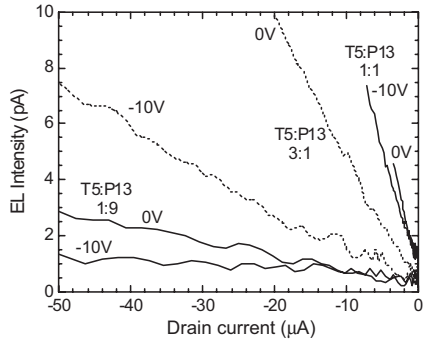

Figure 5. EL intensity as a function of the I_D for bulk-heterojunction composed of T5/P13 ratios of 1:1, 1:3, and 1:9 at gate voltages of 0 and –10 V.

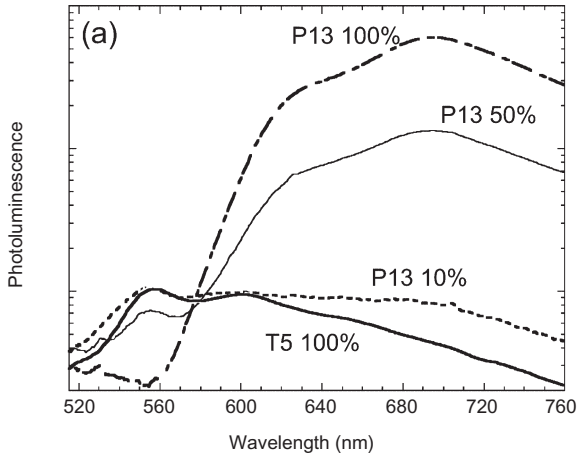

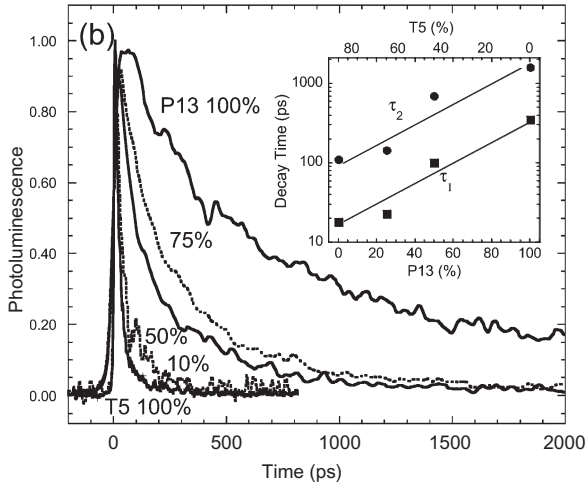

Figure 6. a) Steady-state PL spectra, and b) PL transients of pure P13, co-evaporated thin films of T5 and P13 with different amounts of P13, and pure T5. The inset in (b) shows the extracted decay times assuming biexponential decay. The lines are guides to the eye. Steady-state and time-resolved PL were measured with excitation at 400 nm.

–10 V. The device with a ratio of 1:1 exhibits the steepest slope and the highest EL intensity at a given current, i.e., the highest efficiency. Comparing this result with the mobility values from Figure 4, we see that this ratio also yields the transistor with the best-balanced electron and hole mobilities. The higher the P13 content, the lower the EL intensity and the more unbalanced the charge-carrier mobilities.

To obtain a better understanding of the properties of the bulk-heterojunction transistors, the morphology of the films and the recombination process of the excited states were studied by means of CLSM and time-resolved PL spectroscopy.

Figure 6a shows the PL spectra (on a logarithmic scale) of T5, P13, and co-evaporated T5/P13 films. The PL spectra are measured exciting at 400 nm, where P13 exhibits minimum absorbance. The film with pure P13 emits in the red with a main peak at about 690 nm. The sample with a T5/P13 ratio of 1:1 shows a significantly decreased P13 emission and an additional PL peak from T5 at about 550 nm. The P13 emission almost vanishes when the T5 content is increased further. Roughly two orders of magnitude of the PL intensity are lost by reducing the concentration of P13 from 100 to 25 %. Such a dramatic quenching cannot be justified by the decreased concentration of P13 in the film alone; rather, it is an indication of exciton dissociation upon interaction with T5 molecules.

To further investigate the proposed exciton-dissociation process, the transient PL decay of films with different P13 contents was measured (see Fig. 6b). The PL dynamics of P13 in the bulk-heterojunction films strongly depend on the T5/P13 ratio. The decay of pure P13 films is biexponential, with a first decay time of $\tau_1 \approx 350$ ps and a tail with decay time of $\tau_2 \approx 1.6$ ns. The dynamics of the P13 emission in the co-evaporated films with increasing percentages of T5 become extremely fast, exhibiting decay times up to $\tau_1 \approx 20$ ps and $\tau_2 \approx 100$ ps. Such faster decay times are also typical of neat T5 films, which are characterized by H-type aggregation and for which efficient non-radiative recombination is responsible of the low PL efficiency. The extracted decay times τ_1 and τ_2 as a function of the heterojunction composition are shown in the inset of Figure 6b.

The observed PL dynamics and quenching of the P13 emission can be considered a sign of exciton dissociation by hole

ADVANCED FUNCTIONAL MATERIALS

transfer to the material with the lower ionization potential (T5).

An alternative explanation for the observed P13 lifetime variation, namely, that it is due to energy transfer from P13 to T5, is to be ruled out because the higher energy gap of T5 with respect to that of P13 prevents the process from occurring.

The quenching process competes with exciton recombination and, hence, light emission in bulk heterojunctions. This phenomenon, which is predominant at high T5 concentrations, explains why FET devices with an excess of T5 show no EL emission although the transistor characteristics exhibit clear ambipolar transport.

Further insight into the working mechanism of the device can be obtained from morphological investigations. Figure 7 shows CLSM micrographs of three different bulk-heterojunction compositions in the green and red spectral range.[40] This method to study the morphology and phase composition of the co-evaporated films was chosen because imaging of such films by atomic force microscopy (AFM) is problematic, since P13 tends to move on the substrate[41] upon interaction with the AFM tip. The PL intensity, which is the physical observable in CLSM, is not sensitive to the mechanical properties of the film. Moreover, as the PL emission of T5 and P13 are spectrally separated (T5 peaks at 550 nm and P13 at about 690 nm, see Fig. 6a), it is possible to image the phase separation in the bulk heterojunction by selecting the detection windows to match the emission spectral range of each material. The red and the green channels monitor the P13 and T5 emission, respectively. Note that P13 exhibits a considerably higher PL intensity than the weakly emitting T5.

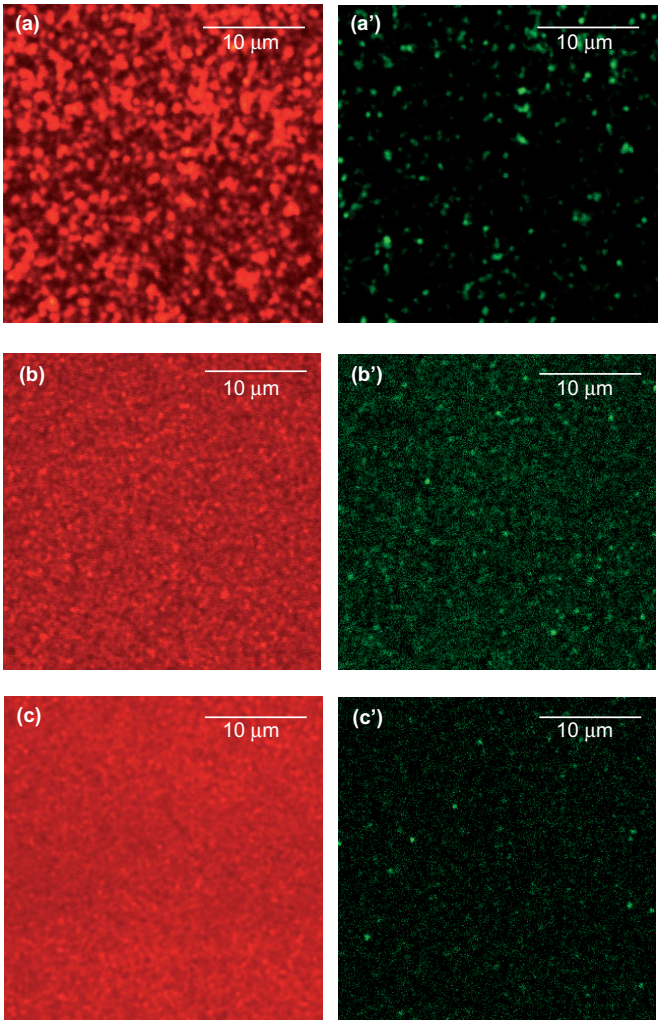

Figure 7. CLSM micrographs of the co-evaporated thin films with different T5/P13 ratios of 3:1 (a,a′), 1:1 (b,b′), and 1:3 (c,c′). The images in (a–c) show the red P13 emission, the images in (a′–c′) show the green channel (T5 emission). The intensity of the red channel in (a) is intensified by a factor of five with respect to the other red-channel images in (b) and (c).

In Figures 7a,a′, the CLSM micrographs for the red and the green spectral ranges of the co-evaporated film with a T5/P13 volume ratio of 3:1 are presented. The morphology of the film is rather inhomogeneous, and the bulk heterojunction is dominated by large T5 clusters ~1 µm in size. In Figures 7b,b′, the CLSM images of the co-evaporated film with a T5/P13 ratio of 1:1 are shown. The film appears rather smooth even though T5 clusters are still visible in the green channel. By increasing the P13 percentage further (Figs. 7c,c′), the surface of the bulk heterojunction appears very smooth, with T5 forming tiny and quite homogeneously distributed clusters in the film.

From the CLSM micrographs, it can be concluded that T5 and P13 do not mix on a molecular scale in the co-evaporated thin films, but form an interconnected network of micro- and nanocrystalline clusters. In particular, the tendency of T5 to form clusters is in good agreement with the observation of thin-film T5 PL spectra in co-evaporated films rather than solution spectra.[42]

Comparing the CLSM information with the electrical characteristics of the bulk-heterojunction LETs with varying compositions of T5 and P13 allows some conclusions on the microscopic structure of the heterojunction and the resulting current percolation to be made. A relative content of 25 % of P13 is sufficient to obtain a continuous path for electrons, resulting in a measurable electron mobility. An equivalent content of T5 is not enough to achieve comparable hole conduction. This can be explained by the different growth mechanisms of the two materials. As T5 tends to form clusters, it is very likely that the percolation threshold to create a continuous pathway for holes is larger than 25 %. In contrast, for the highly surface-mobile P13 molecules, we conclude that the percolation threshold is lower than 25 %. Thus, even diluted concentrations of P13 lead to continuous pathways for electrons in the bulk heterojunction. As a result of the cluster formation, it can be concluded that whether charge separation or light emission is the predominant phenomenon in the T5/P13 bulk heterojunction depends critically on the ratio and dispersion of the two components in the bulk heterojunction.

3. Conclusion

In conclusion, we have presented an ambipolar light-emitting FET based on co-evaporated bulk heterojunction thin films of hole-transporting (T5) and electron-transporting (P13) materi-

als. The electron and the hole mobility, as well as the EL properties, can be tuned over a wide range by changing the composition of the thin film. The highest EL efficiency is obtained in the samples with equal concentrations of T5 and P13, which also exhibit the most balanced electron and hole mobilities. A higher concentration of T5 results in non-light-emitting but still ambipolar FETs. Time-resolved PL spectroscopy revealed that light emission is quenched in devices with an excess of T5 owing to the dissociation of P13 excitons upon interaction with T5 molecules. On the other hand, a lower concentration of T5 results in unipolar n-channel FETs, which are still light-emitting. This is a result of the T5 cluster formation, as revealed by CLSM.

This demonstrates that the bulk-heterojunction approach, which is widely used in organic photovoltaic cells, can be successfully employed to select and tailor the functionality of field-effect devices, including ambipolar charge transport and light emission. By carefully choosing the electronic properties of the molecular systems used to form the bulk heterojunction, their main functionality can be selected to be either photovoltaic or light-emitting.

4. Experimental

Device Fabrication: A heavily doped, n-type Si wafer (doping level: 10^{18} cm^{-3}) with an aluminum back contact acted as the gate electrode and substrate. The gate insulator consisted of a thermally grown SiO_2 layer with a thickness of 150 nm. Prior to processing, the oxidized wafer was cleaned with a standard wet-cleaning procedure, comprising ultrasonic cleaning in acetone and isopropanol. The organic thin-film bulk heterojunction, with a thickness of about 50 nm, was prepared by co-evaporation of T5 and P13 with variable volume ratios. Samples with T5/P13 ratios of 1:3, 1:1, 3:1, and 9:1 have been presented.

The base pressure during the vacuum sublimation of T5 and P13 was 2×10^{-7} mbar (1 mbar = 10^2 Pa), and the deposition rate was kept constant at 0.1 Å s^{-1} for each material. The different volume ratios of T5 and P13 were obtained by reducing the flux of one of the components on the substrate with a mechanical chopper. The indicated relative concentrations of the two materials are nominal; small variations between different depositions could have occurred.

Source and drain Au contacts were thermally evaporated through a shadow mask with a thickness of about 40 nm. The channel length and width of the FET device were 40 and 55.1 mm, respectively.

Electrical Measurements: For electrical characterization, the devices were transferred through air into an argon glove box (<1 ppm O_2, H_2O). The transistor output and transfer characteristics, as well as the photocurrent, were measured with an Agilent 4155C semiconductor parameter analyzer. The mobility values were extracted from the saturated drain current depicted in the transfer characteristics.

Photoluminescence Imaging and Spectroscopy: CLSM was performed with a Nikon Eclipse 2000-E microscope by exciting the sample with the 488 nm Ar^+ laser line. The images were recorded by collecting, point by point, the PL intensity excited by scanning the laser over the sample surface. PL-intensity detection was performed in two spectral ranges, which enabled the PL emission of T5 and P13 to be monitored separately. The first spectral range was centered at 515 ± 20 nm (green channel), and the second at wavelengths greater than 600 nm (red channel). The two spectral ranges were recorded with different amplifications to compensate the low PL efficiency of T5, its low absorption at 488 nm, and the smaller spectral detection window for the T5 emission range (green channel).

PL emission for time-resolved and steady-state measurements was excited by the second harmonic (400 nm) of a Ti:sapphire laser delivering 100 fs pulses. The signal was recorded by a Hamamatsu streak camera with ~2 ps time resolution.

Received: February 21, 2005
Final version: July 4, 2005
Published online: November 30, 2005

[1] C. W. Tang, S. A. VanSlyke, *Appl. Phys. Lett.* **1987**, *51*, 913.
[2] R. H. Friend, R. W. Gymer, A. B. Holmes, J. H. Burroughes, R. N. Marks, C. Taliani, D. D. C. Bradley, D. A. Dos Santos, J. L. Brédas, M. Lögdlund, W. R. Salaneck, *Nature* **1999**, *397*, 121.
[3] S. E. Shaheen, C. J. Brabec, N. S. Sariciftci, F. Padinger, T. Fromherz, J. C. Hummelen, *Appl. Phys. Lett.* **2001**, *78*, 841.
[4] P. Peumans, S. Uchida, S. R. Forrest, *Nature* **2003**, *425*, 158.
[5] L. Edman, M. Pauchard, B. Liu, G. Bazan, D. Moses, A. J. Heeger, *Appl. Phys. Lett.* **2003**, *82*, 3961.
[6] L. Ma, Q. Xu, Y. Yang, *Appl. Phys. Lett.* **2004**, *84*, 4908.
[7] S. Möller, C. Perlov, W. Jackson, C. Taussig, S. R. Forrest, *Nature* **2003**, *426*, 166.
[8] K. Kudo, M. Yamashina, T. Moriizuni, *Jpn. J. Appl. Phys., Part 1* **1984**, *23*, 130.
[9] G. Horowitz, D. Fichou, X. Peng, Z. Xu, F. Garnier, *Solid State Commun.* **1989**, *72*, 381.
[10] D. J. Gundlach, Y. Y. Lin, T. N. Jackson, S. F. Nelson, D. G. Schlom, *IEEE Electron. Device Lett.* **1997**, *18*, 87.
[11] H. Sirringhaus, N. Tessler, R. H. Friend, *Science* **1998**, *280*, 1741.
[12] T. Tsujimura, *SID Int. Symp. Dig. Tech. Pap.* Vol. XXXIV, Book 1, Society for Information Display, San Jose, CA **2003**.
[13] T. N. Jackson, Y. Y. Lin, D. J. Gundlach, H. Klauk, *IEEE J. Sel. Top. Quantum Electron.* **1998**, *4*, 100.
[14] G. H. Gelinck, H. E. A. Huitema, E. Van Veenendaal, E. Cantatore, L. Schrijnemakers, J. B. P. H. Van der Putten, T. C. T. Geuns, M. Beenhakkers, J. B. Giesbers, B.-H. Huisman, E. J. Meijer, E. M. Benito, F. J. Touswlager, A. W. Marsman, B. J. E. Van Rens, D. M. De Leeuw, *Nat. Mater.* **2004**, *3*, 106.
[15] C. D. Sheraw, L. Zhou, J. R. Huang, D. J. Gundlach, T. N. Jackson, M. G. Kane, I. G. Hill, M. S. Hammond, J. Campi, B. K. Greening, J. Francl, J. West, *Appl. Phys. Lett.* **2002**, *80*, 1088.
[16] P. Mach, S. J. Rodriguez, R. Nortrup, P. Wiltzius, J. A. Rogers, *Appl. Phys. Lett.* **2001**, *78*, 3592.
[17] A. Hepp, H. Heil, W. Weise, M. Ahles, R. Schmechel, H. von Seggern, *Phys. Rev. Lett.* **2003**, *91*, 157 406.
[18] C. Santato, R. Capelli, M. A. Loi, M. Murgia, F. Cicoria, V. A. L. Roy, P. Stallinga, R. Zamboni, C. Rost, S. F. Karg, M. Muccini, *Synth. Met.* **2004**, *146*, 329.
[19] M. Ahles, A. Hepp, R. Schmechel, H. von Seggern, *Appl. Phys. Lett.* **2004**, *84*, 428.
[20] T. Sakanoue, E. Fujiwara, R. Yamada, H. Tada, *Appl. Phys. Lett.* **2004**, *84*, 3037.
[21] B. Crone, A. Dodabalapur, Y.-Y. Lin, R. W. Filas, Z. Bao, A. LaDuca, R. Sarpeshkar, H. E. Katz, W. Li, *Nature* **2000**, *403*, 521.
[22] E. J. Meijer, D. M. De Leeuw, S. Setayesh, E. van Veenendaal, B.-H. Huisman, P. W. M. Blom, J. C. Hummelen, U. Scherf, T. M. Klapwijk, *Nat. Mater.* **2003**, *2*, 678.
[23] M. Freitag, J. Chen, J. Tersoff, J. C. Tsang, Q. Fu, J. Liu, P. Avouris, *Phys. Rev. Lett.* **2004**, *93*, 076 803.
[24] N. Karl, *Synth. Met.* **2003**, *133*, 649.
[25] C. D. Dimitrakopoulos, P. R. L. Malenfant, *Adv. Mater.* **2002**, *14*, 99.
[26] a) R. J. Chesterfield, C. R. Newman, T. M. Pappenfus, P. C. Ewbank, M. H. Haukaas, K. R. Mann, L. L. Miller, C. D. Frisbe, *Adv. Mater.* **2003**, *15*, 1278. b) T. Yasuda, T. Tsutsui, *Chem. Phys. Lett.* **2005**, *402*, 395.
[27] A. Dodabalapur, H. E. Katz, L. Torsi, R. C. Haddon, *Appl. Phys. Lett.* **1996**, *68*, 1108.

[28] W. Geens, S. E. Shaheen, C. J. Brabec, J. Portmans, N. S. Sariciftci, *AIP Conf. Proc.* **2000**, *544*, 516.
[29] C. Rost, D. J. Gundlach, S. Karg, W. Riess, *J. Appl. Phys.* **2004**, *95*, 5782.
[30] N. Corcoran, A. C. Arias, J. S. Kim, J. D. MacKenzie, R. H. Friend, *Appl. Phys. Lett.* **2003**, *82*, 299.
[31] M. M. Alam, C. J. Tonzola, S. A. Jenekhe, *Macromolecules* **2003**, *36*, 6577.
[32] a) A. C. Arias, J. D. MacKenzie, R. Stevenson, J. J. M. Halls, M. Inbasekaran, E. P. Woo, D. Richards, R. H. Friend, *Macromolecules* **2001**, *34*, 6005. b) F. Yang, M. Shtein, S. Forrest, *Nat. Mater.* **2005**, *4*, 37.
[33] K. Tada, H. Harada, K. Yoshino, *Jpn. J. Appl. Phys., Part 1* **1996**, *35*, L944.
[34] C. Rost, S. Karg, W. Riess, M. A. Loi, M. Murgia, M. Muccini, *Appl. Phys. Lett.* **2004**, *85*, 1613.
[35] M. Melucci, M. Gazzano, G. Barbarella, M. Cavallini, F. Biscarini, P. Maccagnani, P. Ostoja, *J. Am. Chem. Soc.* **2003**, *125*, 10 266.
[36] P. R. L. Malenfant, C. D. Dimitrakopoulos, J. D. Gelorme, L. L. Kosbar, T. O. Graham, A. Curioni, W. Androni, *Appl. Phys. Lett.* **2002**, *80*, 2517.
[37] D. Jones, M. Guerra, L. Favaretto, A. Modelli, M. Fabrizio, G. Distefano, *J. Phys. Chem.* **1990**, *94*, 5761.
[38] M. Hiramoto, K. Ihara, H. Fukusumi, M. Yokoyama, *J. Appl. Phys.* **1995**, *78*, 7153.
[39] M. A. Lampert, P. Mark, in *Current Injection in Solids* (Eds: H. G. Booker, N. DeClaris), Academic Press, New York **1970**.
[40] M. A. Loi, E. Dacomo, F. Dinelli, M. Murgia, R. Zamboni, F. Biscarini, M. Muccini, *Nat. Mater.* **2005**, *4*, 81.
[41] C. W. Struijk, A. B. Sieval, J. E. J. Dakhorst, M. van Dijk, P. Kimkes, R. B. M. Koehorst, H. Donker, T. J. Schaafsma, S. J. Picken, A. M. van de Craats, J. M. Warman, H. Zuilhof, E. J. R. Sudhölter, *J. Am. Chem. Soc.* **2000**, *122*, 11 057.
[42] M. A. Loi, A. Mura, G. Bongiovanni, C. Botta, G. Di Silvestro, R. Tubino, *Synth. Met.* **2001**, *121*, 1299.